Hydrogen in Pd/Nb multilayers

Q. M. Yang, G. Schmitz, S. Fähler, H. U. Krebs, and R. Kirchheim
Institut für Metallphysik, Universität Göttingen, Hospitalstrasse 3/7, 37073 Göttingen, Germany
(Received 19 March 1996)

Several Pd/Nb multilayers with various modulation periods have been prepared by laser deposition. Hydrogen was doped into the samples electrolytically or from the gas phase. The elastic response of the multilayers upon absorption of hydrogen, their relaxation and phase separation were studied by x-ray diffraction in reflectional, transmissional, and tilting geometries. It was found that the elastic expansion of the Nb layers after the first two cycles of hydrogen loading and unloading can be described well by a model allowing expansion in one dimension only. Phase separation is observed in the Nb layers as well as in the Pd layers. The phase separation is believed to be initiated by a plastic instability of the film due to hydrogen incorporation. The relaxation and change of strain mode in the multilayers due to hydrogen loading and unloading are discussed concerning the possible defects in the sample formed during sample preparation. [S0163-1829(96)01834-6]

I. INTRODUCTION

The study of hydrogen in thin films, superlattices, and multilayers has been the subject of recent theoretical and experimental interest.[1–8] Fundamentally, the study of H in superlattices and thin films is motivated by the possibility of new phenomena related to the reduced dimensionality. The pioneering work of Miceli and Zabel and their co-workers focused on the critical phenomena of H in strain and composition modulated superlattices and has revealed many novel features.[1–4] Later, the work on Mo/V superlattices of Hjörvarsson and his co-workers has emphasized the effects of electron transfer at Mo/V boundaries on H absorption in V layers.[6,7] In such work, H is taken as a probe in the host metals to detect the local elastical and electronical state around the H atom.[8] Practically, on the other hand, H was reported to play an important role as an effective ''cold annealing'' agent to improve the quality of thin epitaxial films.[9] Also, H can be one component in thin films or multilayers leading to different lattice parameters and different structures of the host. This may be accompanied by changes of magnetism, conductivity, optical and mechanical properties of the host films. Some attempts have been made in improving the magnetism of Fe/Ce and Fe/Nb multilayers.[10,11] The effect of H on superconductivity and magnetism of high-T_c materials is another active topic of this kind.[12] From the view point of materials science, the study of H in multilayers may improve the understanding of H in structural composite materials. Interfaces in composite materials are critical to their mechanical properties and, unfortunately, they are also generally favorite positions for H trapping. The thermodynamics and diffusion of H could play a very important role in determining the mechanical properties of such materials. Another possible potential of the study of H in multilayers could be the conventional field of hydride applications. H purification, isotope separation, and H sensoring, for instance, may find new solutions based on multilayer systems. These systems may provide a combination of different requirements in one material package to carry out a task, which cannot be done by bulk materials or by single element films.

In the present work, results on H in Pd/Nb multilayers are presented, focusing on fundamentals of the kinetic and thermodynamic behavior of H in this special system. Both bulk systems, H-Pd and H-Nb, are well-studied ones facilitating the interpretation of the results on thin films and multilayers. So far, only a few results on Nb and Pd thin film or multilayer systems have been reported.[13–20] Although no consensus is accepted about the interpretation of the results, a lowered critical temperature and narrowed coexistence region were found generally in thin Pd films compared to the bulk.[13–16] In Nb thin films, greatly enhanced solubility of H was reported by Moehlecke *et al.*,[17] based on the relation of lattice parameters and H content in bulk materials. Similar results were reported for Nb in Pd/Nb multilayers in the same work. The authors claimed that the expansion of the film is uniform in all directions and similar to that in bulk materials with free boundaries. Later a direct measurement of H content in such thin films were carried out by Steiger *et al.*[18] and Reimer *et al.*[19] using the nuclear reaction method of $^{1}\mathrm{H}(^{15}\mathrm{N},\alpha\gamma)^{12}\mathrm{C}$. It was found that the hydrogen concentration in thin Nb films is lower than that in the bulk at the same equilibrium H pressure. The high expansion in the film normal direction is explained by the fact that only one-dimensional expansion is allowed in this direction due to the in-plane constraints.[20] Miceli *et al.*[20] also claimed that the phase separation might be initiated by plastic instabilities of the film. From the above studies, however, very limited data about the relation between lattice parameter and H content have been obtained except that reported by Reimer *et al.*[19] A very large expansion of out-of-plane parameters, more than three times higher than expected from the one-dimensional expansion model was observed. Since the data were collected in a small concentration range (0–2 at. %), more work may be needed mainly at higher H concentration in order to confirm this.

In the present work, the hydrogen concentration will be varied in a wide range by electrolytical doping and the lattice parameters are obtained by immediate x-ray diffraction (XRD) measurement between the doping steps. The phase transformation will be monitored by XRD and also by electromotive force (EMF) measurements.

II. EXPERIMENTAL DETAILS

Specimens of Pd/Nb multilayers with various modulation lengths (double-layer thickness will be denoted by Λ) have been prepared by pulsed laser deposition in an ultrahigh vacuum chamber as described earlier.[21,22] The multilayers were deposited on single-crystalline silicon substrates. The bilayer thickness was chosen larger than 12 nm so that in XRD patterns the Nb and Pd reflections are separated and no satellite reflections from the layered structure occurred. Both the bottom and top layers of the multilayers are Pd layers in order to protect the Nb layers and to get fast kinetics of hydrogen absorption and desorption. The Nb and Pd layers show a strong texture with Nb{110} and Pd{111} planes parallel to the film surface. Only the interplane spacings of these two planes were obtained by conventional XRD in reflectional geometry. Hydrogen was doped into the sample step by step electrolytically using an electrolyte of phosphoric acid in glycerin at room temperature.[23] From thermodynamic data of bulk Nb-H and Pd-H systems,[24] within the low concentration range and at room temperature, the solubility of H in Nb is 2.8×10^5 times larger than that in Pd at the same H_2 pressure. Therefore, nearly all H is located in Nb layers at the beginning of loading. The hydrogen concentration in Nb layers is thus calculated by Faraday's law before significant hydrogen is absorbed in Pd layers and bubbling of molecular H_2 occurs. The out-of-plane lattice parameter of Nb and Pd are monitored by XRD in the intervals between two consecutive loading steps.

Hydrogen is believed to be removed from the multilayer by formation of water at the top Pd layer according to a catalyzed reaction with oxygen from the air. The rate of this reaction appears to be strongly dependent on the surface condition and treatment history of the sample. For the samples used in the measurements described above, the hydrogen in the Nb layers was rather stable. It stayed inside the specimens several days to several weeks in air or in vacuum under the current surface conditions at temperatures below 80 °C. At room temperature, where the XRD was carried out, the change of lattice parameters of Nb in 12 h was less than 5% of the overall change. A temperature above 200 °C was necessary to remove all the hydrogen within 8 h. The in-plane lattice parameters of the films were obtained by XRD in transmissional geometry or by a four-axis diffractometer (''Philips X'pert MPD''). Due to the limited intensities a long measuring time was needed in collecting the in-plane parameters. Unfortunately the specimens prepared with a geometry suitable for the four-axis diffractometer lost their hydrogen very quickly. Thus, these measurements were only possible before loading and after unloading of hydrogen. Therefore, only the film relaxation is monitored by the in-plane parameter measurement.

The measurements of the chemical potential were carried out using the double-cell described previously.[23] In order to measure the potential of the film at the side opposite to the doping one, the multilayer was deposited on a pure Pd substrate 12.5 μm in thickness. An additional Si support provided sufficient mechanical stability. The complete sample package is sketched in Fig. 1. The H content in the multilayer is calculated by comparing the amount of H doped into the package with that doped into a pure Pd substrate for the same EMF.

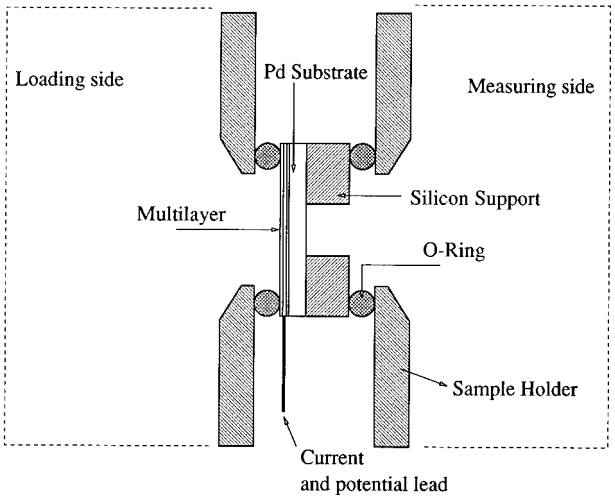

FIG. 1. Schematic drawing of the multilayer sample and Pd substrate for EMF measurement. The Si wafer contains a hole and provides the necessary support for the thin Pd substrate.

III. EXPERIMENTAL RESULTS AND DISCUSSION

A. The elastic response of Nb/Pd multilayers at low hydrogen concentration

Figure 2 shows the XRD patterns of a Pd/Nb multilayer taken in a conventional reflection geometry for several different hydrogen loading states. The sample has an overall thickness of 580 nm with 20 bilayers and a top layer of Pd. The bilayer thickness is 28.3 nm with an atomic ratio of Pd/Nb=46.9/53.1. In Fig. 2(a), results of the first loading cycle starting from the as-prepared sample are presented. Subsequently the specimen was degassed by an annealing treatment at 200 °C for 14 h in an argon atmosphere and then loaded again. Results of this second loading are shown in Fig. 2(b) and of a further third loading cycle in Fig. 2(c). In all three cycles the peak of Nb (110) shifts to the left, when the sample is loaded with small amounts of H up to a concentration of about 20 at. % hydrogen in the Nb layers. Increasing the H content gives rise to the occurrence of another phase with larger interplane spacings (denoted by β_{Nb} in the figure) and its amount increases with total H content. Finally, the first phase disappears and all of the Nb layers consist of the second phase. It is also noted that the Pd (111) peak does not shift until the Nb layers are saturated. Thus, the hydrogen content in Nb layers can be calculated by assuming that all of the H electrochemically produced is located in Nb layers until they are saturated. When the sample is charged to a state where molecular H is formed at the Pd surface and consequently gaseous hydrogen bubbles out of the electrolyte into the air, a second hydride phase (β_{Pd}) is formed in the Pd layers too. Because of the hydrogen losses to the atmosphere the content inside the specimen cannot be quantified for this late charging state.

To begin with, in this section only the elastic response of single-phase Nb layers on charging with small amounts of hydrogen should be discussed. The interplane spacing Nb

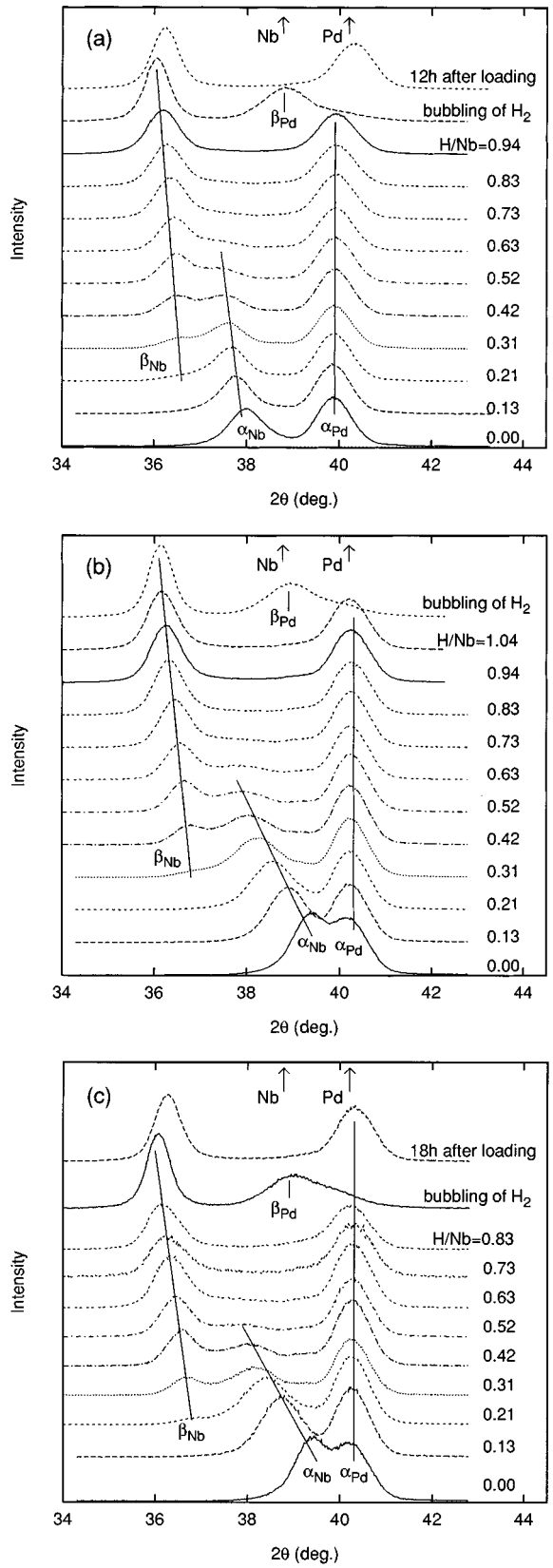

FIG. 2. XRD spectra (using Cu $K\alpha$ radiation) of Pd/Nb multilayers with a layer periodicity of $\Lambda = 28.3$ nm in reflectional geometry. (a) First loading of the as-prepared sample with different H concentrations given in the figure. (b) Second loading after degassing at 200 °C for 12 h. (c) Third loading after degassing again. The peak positions for bulk Nb and bulk Pd are marked by small arrows in the upper part.

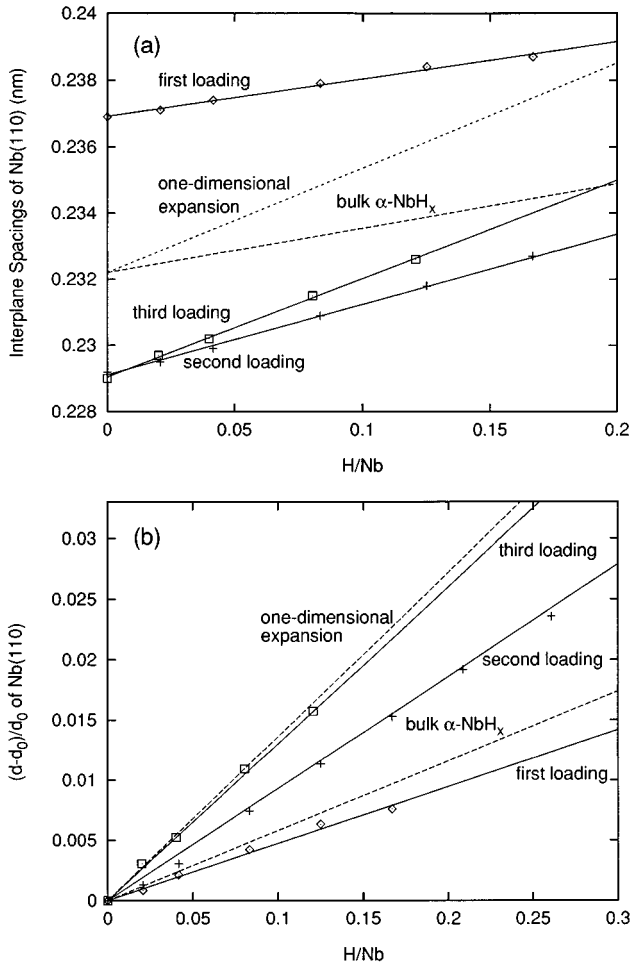

FIG. 3. Interplanar spacing of Nb(110) vs H content in Pd/Nb multilayers with $\Lambda = 28.3$ nm for low concentrations within the α phase. (a) Absolute and (b) relative changes. Solid lines connecting the experimental points are results of a linear fit.

(110) ($d_{\mathrm{Nb}(110)}$) at low H contents is shown in Fig. 3(a). Figure 3(b) gives the relative change $(d-d_0)/d_0$ with d_0 being the initial values without hydrogen. It is seen that in the as-prepared sample $d_{\mathrm{Nb}(110)}$ is 2.0% larger than the value of bulk Nb and increases linearly with H content. After annealing the sample, $d_{\mathrm{Nb}(110)}$ dropped to a value which is 1.3% smaller than the bulk value. During the second cycle, the interplane spacing increases linearly again, but with a larger slope compared to the first cycle. The third cycle gives similar results as the second one with a slightly larger slope. Afterwards, further charge-discharge and annealing has no significant effects on the slope and the initial value of $d_{\mathrm{Nb}(110)}$. In bulk materials, the host metals expand linearly with hydrogen content. For Nb the following relation is held for the interplane spacing of any crystalline plane:[25]

$$\left(\frac{\Delta d}{d_0}\right)_b = \frac{1}{3}\left(\frac{\Delta V}{V_0}\right)_b = 0.058 X_H , \tag{1}$$

where X_H is the atomic ratio of H to Nb and $(\Delta d/d_0)_b$ and $(\Delta V/V_0)_b$ are the relative change of interplane spacings and the volume for the bulk material, respectively. For thin films

clamped on a substrate, there may be different cases depending on the constraints imposed by the substrate.

(1) One-dimensional expansion: This is the case of complete lateral clamping of the film on the substrate. In Pd/Nb multilayers, the lateral expansion of Nb is also constrained by the neighboring Pd layers which do not expand because only Nb layers accommodate the H at the beginning of the loading. In this case, the expansion of the Nb layers in normal direction may be described by[19]

$$\frac{\Delta d}{d_0}=\left(1+\frac{C_{11}+3C_{12}-2C_{44}}{C_{11}+C_{12}+2C_{44}}\right)\left(\frac{\Delta d}{d_0}\right)_b \tag{2}$$

if its elastic anisotropy is considered, and by

$$\frac{\Delta d}{d_0}=\left(1+\frac{2\nu}{1-\nu}\right)\left(\frac{\Delta d}{d_0}\right)_b, \tag{3}$$

if the material is considered to be isotropic. Here C_{ij} in Eq. (2) and ν in Eq. (3) are elastic constants and Poisson's ratio of the material, respectively. Equations (2) and (3) are obtained by the following procedure.[19] First, the film is allowed to expand in all directions as in bulk materials and second, the film is biaxially compressed to its original lateral dimensions while keeping the normal direction free. The second step adds an extra expansion in the normal direction according to the elasticity of the material. Simple addition of the two expansions in the normal direction is assumed to give the overall expansion in the normal direction. For Nb the following value may be obtained by Eq. (2) and the elastic constants of Nb:[26]

$$\frac{\Delta d}{d_0}(110)=0.136X_H \tag{4}$$

and if neglecting the small anisotropy of Nb, we have, from Eq. (3) and a Poisson's ratio of $\nu=0.397$:

$$\frac{\Delta d}{d_0}(110)=0.134X_H. \tag{5}$$

Because of the small quantitative difference between the anisotropic and the isotropic model, the isotropic approximation will be further used throughout this paper to avoid lengthy formulas.

(2) Constraint free: This could be reached by a complete relaxation of strains at the interfaces. The corresponding expansion in the normal direction of the film is the same as in the bulk given by Eq. (1).

(3) Semi-constraint: In this case the constraint between the layers and the substrate is partly relaxed. The expansion in the normal direction is expected to be in between the two extremes above.

In Fig. 3(b) both, the one-dimensional expansion limit, Eq. (4), and the constraint free expansion, Eq. (1), are shown together with the experimental results. It is seen that the expansion of Nb in as-prepared samples is even smaller than that of bulk Nb, whereas samples after the second cycle exhibit an expansion which is in agreement with the one-dimensional expansion limit within the experimental error range. From these results, it is inferred that, after two charge-discharge cycles, the multilayers come to a state where relaxation has been completed and the expansion in the Nb layers is completely constrained by the substrate and the neighboring Pd layers in the composition range concerned. More importantly, these results show that the elastic behavior of thin Nb films in Pd/Nb multilayers is similar to bulk Nb, because the simple model, Eq. (3), based on the elastic behavior of the bulk Nb-H system, describes the experimental results of multilayers quite well.

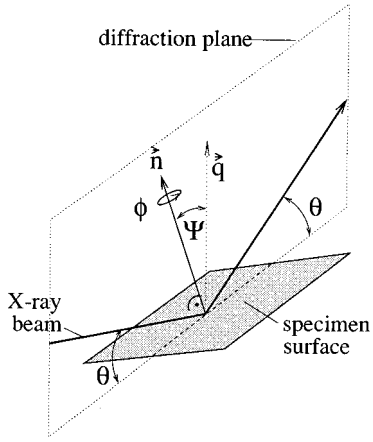

FIG. 4. Beam geometry of the four-axis diffractometer with definition of the angles mentioned in the text: $\vec{n}$ normal of the film surface, $\vec{q}$ scattering vector, ψ angle between $\vec{n}$ and $\vec{q}$, ϕ angle of film rotation around axis $\vec{n}$.

Regarding the first two cycles, the abnormal elastic response of the film upon absorption of H seems to be due to a relaxation process within the film. The case of semiconstraint may be ruled out by the fact that the normal expansion of the as-prepared sample is not in between that of the bulk and that of the one-dimensional expansion limit, as expected in this case according to the discussion above.

From Fig. 3(b), it is seen that the interplane spacing of (110) Nb is smaller than the bulk value after the first loading-unloading cycle. It seems that the relaxation process introduces an expansion in the film plane and thus a contraction in the normal direction of the film. If this takes place during the first loading process, the contraction in the normal direction will counteract the expansion of the lattice due to absorption of hydrogen, which makes a net expansion of the lattice smaller than expected. In the next section, the change of in-plane lattice parameters will be determined before and after a loading-unloading cycle, to see whether the above assumption is true.

B. Relaxation of the multilayers upon hydrogen loading and unloading

The geometry of the four-axis diffractometer is schematically shown in Fig. 4. The sample can rotate with an axis along the normal of the film surface. The angle of the rotation is denoted as ϕ. When the diffraction angle 2θ is fixed at a position where Bragg diffraction occurs, the change of ϕ does not influence the intensity of diffraction, indicating that no texture is formed in the film plane. The other angle which can be adjusted is ψ. It is the angle between the scattering vector and the film normal vector. If the normal of a

TABLE I. Lattice strains in the normal direction of the indexed planes. First cycle, after first loading and unloading by annealing at 200 °C for 12 h; second cycle, after second loading and unloading by annealing at 200 °C for 12 h; for definitions of ϵ and $\Delta\epsilon$, see text.

				Niobium			
Strains (%)	$\epsilon(110)$	$\epsilon(011)$	$\epsilon(112)$	$\Delta\epsilon$ (110)	$\Delta\epsilon(\bar{1}10)$	$\Delta\epsilon$ (001)	$\Delta\epsilon_0$
ψ (degree)	0	60	54.7	0	90	90	
As-prepared	1.94	0.02	0.46	1.55	−1.68	−0.67	0.39
First cycle	−1.57	0.89	0.50	−1.91	1.71	1.19	0.34
Second cycle	−1.83	0.86	0.51	−2.06	1.68	1.45	0.23
				Palladium			
Strains (%)	$\epsilon(111)$	$\epsilon(\bar{1}3\bar{1})$	$\epsilon(\bar{1}11)$	$\Delta\epsilon(111)$	$\Delta\epsilon(\bar{2}11)$	$\Delta\epsilon(0\bar{1}1)$	$\Delta\epsilon_0$
ψ (degree)	0	80	70	0	90	90	
As-prepared	0.56	−0.11	−0.15	0.40	−0.39	−0.25	0.16
First cycle	−0.25	0.87	0.98	−0.69	0.70	0.40	0.44
Second cycle	−0.39	0.80	0.93	−0.73	0.75	0.41	0.34

crystalline plane in the film has an angle of ψ to the film normal, the condition of the Bragg diffraction of this plane requires that the scattering vector is aligned along its plane normal. This can be performed by tilting the sample by an angle equal to ψ.

Including the results obtained at $\psi=0$, all experimental results on lattice strains are collected in Table I. The strain ϵ values in Table I are obtained directly from XRD data via relative changes of lattice spacings $(d-d_0)/d_0$. $\Delta\epsilon$ values are strains in mutually perpendicular directions calculated from elasticity after separating the isotropic expansion ϵ_0, which is due to defects formed during sample preparation or hydrogen loading. An example of the calculation for the case of Nb is given below:

$$\epsilon(110)=\Delta\epsilon(110)+\Delta\epsilon_0, \tag{6}$$

$$\epsilon(011)=[\Delta\epsilon(110)+\Delta\epsilon_0]l^2+[\Delta\epsilon(\bar{1}10)+\Delta\epsilon_0]m^2 +[\Delta\epsilon(001)+\Delta\epsilon_0]n^2, \tag{7}$$

$$\epsilon(112)=[\Delta\epsilon(110)+\Delta\epsilon_0]l'^2+[\Delta\epsilon(\bar{1}10)+\Delta\epsilon_0]m'^2 +[\Delta\epsilon(001)+\Delta\epsilon_0]n'^2, \tag{8}$$

$$\Delta\epsilon(110)=-\frac{\nu}{E}[\sigma(\bar{1}10)+\sigma(001)], \tag{9}$$

$$\Delta\epsilon(\bar{1}10)=\frac{1}{E}[\sigma(\bar{1}10)-\nu\sigma(001)], \tag{10}$$

$$\Delta\epsilon(001)=\frac{1}{E}[\sigma(001)-\nu\sigma(\bar{1}10)], \tag{11}$$

where E is Young's modulus, σ's are stresses in the corresponding direction, l, m, n are cosines of (011) to (110), ($\bar{1}10$), and (001) and l', m', n' cosines of (112) to (110), ($\bar{1}10$), and (001), respectively. It is seen from Table I that both Nb and Pd in the as-prepared layers are expanded in the film normal direction [positive $\Delta\epsilon(110)$ of Nb and $\Delta\epsilon(111)$ of Pd] and contracted in the film plane [negative $\Delta\epsilon(\bar{1}10)$ and $\Delta\epsilon(001)$ of Nb and $\Delta\epsilon(\bar{2}11)$ and $\Delta\epsilon(0\bar{1}1)$ of Pd]. After loading and unloading by annealing, the strain mode of the film in its normal direction and its in-plane direction are reversed. In its normal direction, the film becomes contracted from an originally expanded state, while in plane the contraction is reversed to an expansion. After the second cycle, no significant difference is observed except quantitative adjustment. It is clear that the ''relaxation'' process of the film leads to a contraction in its normal direction and expansion in the film plane, answering the question raised in the last section. It is shown that the smaller expansion of the film in its normal direction upon the first absorption of H is indeed resulting from a counteracting of a volume increase due to H and a contraction of the film in the normal direction due to its ''relaxation.'' We use quotation marks to emphasize the fact that the film is not really relaxed but strained in a different mode.

Regarding possible mechanisms of the above relaxation process, more detailed work is in progress. In this work, it will be briefly discussed only. Laser deposition is used in this work to prepare the multilayers. One of the features of this technique is that the energy of the deposited atoms and ions is very large [up to more than 100 eV (Ref. 27)]. Such an energy level is above the threshold for the formation of Frenkel defects in metals and therefore, defects like interstitials and vacancies may be formed during the preparation process, as in high energy particle irradiated metals.[28] These defects may anneal immediately after their formation at grain boundaries, layer interfaces, or aggregate into dislocation loops. Because those defects have their own free volumes, their annihilation at grain boundaries perpendicular to the film surface or aggregation into dislocation loops in crystalline planes not parallel to the film surface[29,30] will intend to enlarge or decrease the lateral dimension of the film. Since the film is constrained by the substrate and previously formed layers, corresponding stress will be developed between film and substrate to account for this change of dimension. From Table I, it is seen that the strain in an as-prepared sample is negative in its lateral directions, indicating an intention of lateral compression due to preparation defects. Therefore, it

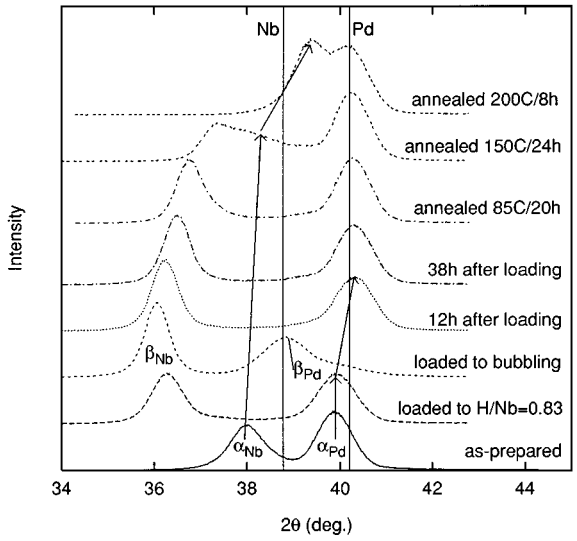

FIG. 5. XRD spectra (using Cu $K\alpha$) of Pd/Nb multilayers after different treatments. The peak positions for bulk Nb and bulk Pd are marked by vertical lines.

is reasonable to assume that these defects are mainly produced by interstitials which have positive free volume. From the extent of strains in Nb and Pd layers, the concentration of defects in Nb should be much higher than in Pd.

Next we discuss the temperature at which the relaxation take places. Figure 5 presents the XRD patterns in reflectional geometry for the sample before and after hydrogen loading and after annealing at various temperatures. First, let us focus on the change of the Pd lattice parameters. It is seen that the Pd (111) peak keeps a constant position during loading before Pd hydride is formed (see also Fig. 2), indicating that hydrogen diffusion through the Pd layer (into the Nb layer) does not help its relaxation. However, absorption of H in Pd layers itself and formation of the Pd hydride phase and thereafter the release of H into air at room temperature let the interplane spacing of Pd(111) decrease and finally become smaller than its bulk value. Therefore, it is concluded that the relaxation in Pd layers can proceed at room temperature via absorption of H and phase separation. Whereas, relaxation without hydrogen will not occur by annealing at a temperature below 375 °C. Above 375 °C a reaction between Pd and Nb takes place.

In Nb layers, however, it is not clear whether a complete relaxation takes place due to the loading and subsequent unloading of H at room temperature or whether it is initiated by the later annealing at 200 °C, as the H cannot be removed completely at room temperature. From results of other samples, where H desorbes in a few hours at room temperature, it is found that the final out-of-plane lattice parameters are smaller than the as-prepared sample but still bigger than the bulk. What can be inferred is that the relaxation starts at room temperature during loading and unloading of H, as indicated by the smaller expansion of (110) Nb for the first two loading cycles.

Another experiment was carried out in order to check whether the phase separation in Nb is the main reason for a complete relaxation of strains in the as-prepared samples. The as-prepared sample was loaded with gaseous H at a temperature of 200 °C which is higher than the critical temperature for phase separation. The interplane spacing of Nb(110) is monitored by XRD *in situ* during loading. After Nb is saturated with H at a pressure of 10 mbar, the lattice spacing of Nb(110) reached a value which corresponds to the second phase when loaded electrochemically at room temperature. Then the sample is degassed also at 200 °C by pumping the chamber to a base pressure of 10^{-6} mbar. It was found that the final interplane spacing of Nb(110) is only about 0.35% smaller than that of the as-prepared one and still larger than the bulk value. A complete relaxation is not reached, although the Nb layers were at a similar stress level and at the same temperature at which the annealing of the samples doped at room temperature is performed. It may be concluded from this observation that the relaxation of preparation strains, or the change of strain mode in the film, is greatly facilitated by phase separation.

Another interesting point related to the above experiment is noted. From Fig. 3(b), it is seen that the difference of expansion of Nb(110) between the first and third loading is about 0.012 at $X_H=15\%$. If this is considered to be the part of strain relaxed by extra stress due to H, the part relaxed by loading from the gaseous phase should be larger, as more stress [due to a larger d value of Nb(110)] has been introduced. Nevertheless, as is mentioned above, the strain relaxed by gaseous loading and unloading is only 0.0035. An assumption may explain this phenomenon, i.e., the strain relaxed by H absorption without phase separation is elastically reversible and can be restored to some extent when H is released. The linearity of the relaxation in this range also supports such an assumption.

Such a process, being elastic and reversible, could be exemplified by the following picture. Suppose that a dislocation loop on a (110) plane with a Burgers vector of $(a/2)[111]$ is formed by aggregation of interstitials, as observed in irradiated bcc metals.[28] If the perfect dislocation of $(a/2)[111]$ dissociates then via the reaction

$$\frac{a}{2}[111]=\frac{a}{8}[110]+\frac{a}{4}[112]+\frac{a}{8}[110], \qquad (12)$$

three partial dislocations and two stacking fault ribbons are formed. This process is accompanied by a decrease of the total energy and a contraction of the lattice perpendicular to the fault plane. According to Amelinckx,[31] this process can be schematically described as in Fig. 6. Since the film of the as-prepared sample has an in-plane compressive stress and strain, the above dissociation with a contraction in lateral direction of $[\bar{1}10]$ may be enhanced and make the fault ribbons wider than in its stress free state. When H is incorporated in the lattice, the intention of the lattice expansion and the constraint of the substrate introduce extra compressive stress in the film plane. This extra stress will force the faults to extend further and a new equilibrium between the fault width and strain is established. The contraction related to this further dissociation, therefore, offsets the expansion due to H. When H is released, the stacking fault width-strain equilibrium and thus the strain state of the film may be restored.

In fact, a reversible elastic process like the above could also be realized by dislocation dissociation having expansion

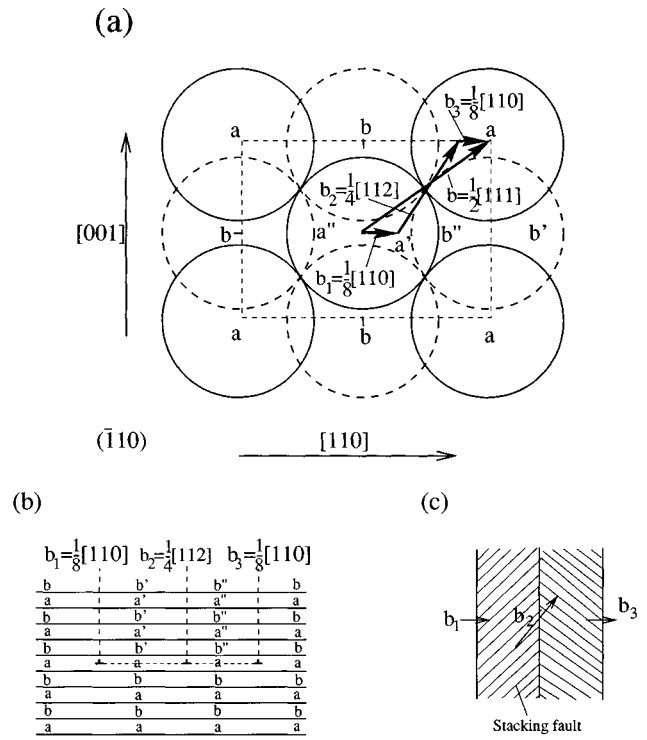

FIG. 6. Schematic drawing of $(a/2)[111]$ dislocation dissociation on a (110) plane (Ref. 31). (a) Atom positions, a and b, of two successive {110} layers; a' and a'' (and b' and b'') are possible quasiequilibrium faulted positions of atoms. (b) The arrangement of layers in the extended dislocations. (c) Geometry of the stacking fault ribbons.

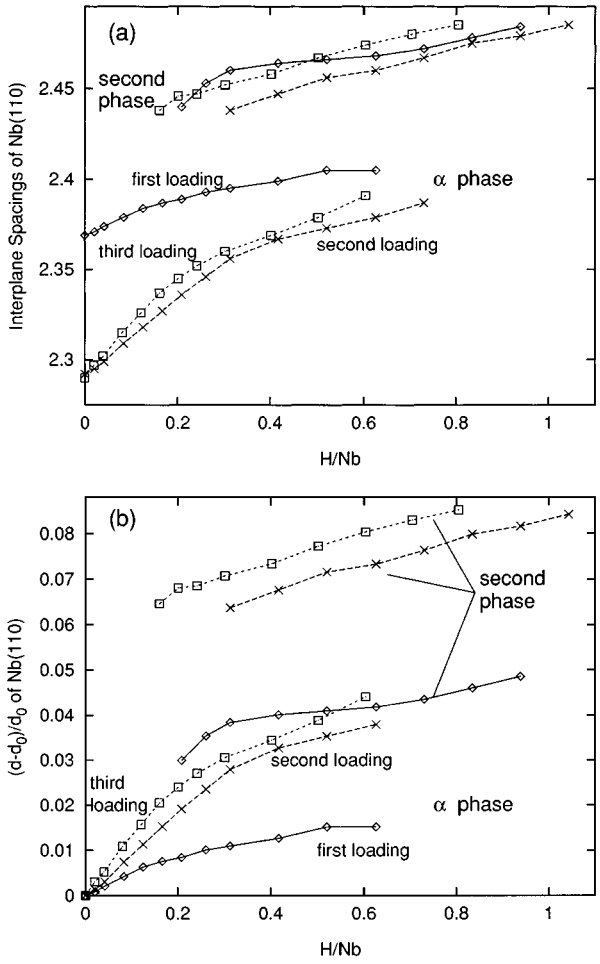

FIG. 7. Interplanar spacing of Nb(110) vs H content in Pd/Nb multilayers with $\Lambda = 28.3$ nm for the whole concentration range. (a) Absolute and (b) relative changes.

in faulted planes. There the incorporation of H could result in shrinking of the stacking faults to offset the expansion of lattice due to H.

When the H concentration reaches a critical value, phase separation occurs. No matter whether the phase separation is initiated by a plastic instability first,[20] a plastic flow due to phase separation itself and the movement of phase boundaries will help to eliminate the intrinsic strain in the as-prepared sample and accommodate further the strain due to the formation of a second phase. When the film is degassed by annealing, an intention of contraction of the film may introduce a tensile stress in the lateral direction of the film due to the constraint of the substrate and neighbored layers. Therefore, an in-plane expansion may be developed in the film, accounting for the experimental results.

C. Phase transformation in Nb layers

Phase separation has been observed in multilayers with bilayer thicknesses Λ of 63 nm (Nb 40.9 nm), 32.6 nm (Nb 16.6 nm), 28.3 nm (Nb 13.6 nm), and 21 nm (Nb 10.7 nm), besides one exception with $\Lambda = 26.6$ nm (Nb 6.2 nm). The XRD patterns of one of the above sample ($\Lambda = 28.3$ nm) upon H absorption have been presented in Fig. 2. The corresponding lattice parameters of Nb(110) are shown in Fig. 7. The EMF of H in the sample with $\Lambda = 21$ nm is shown in Fig. 8 for the third loading.

As shown in Fig. 2 and Fig. 7, an extra peak at the left of the shifted Nb(110) peak occurred when the H content reaches a value of H/Nb = 0.21, 0.31, and 0.16 for the first, second, and third loadings, respectively. This feature of having two peaks is rather stable and remains after annealing at 150 °C for 24 h. As shown by the time lag technique,[32] the diffusion of H in Pd/Nb multilayers is quite fast, because it takes only several seconds for hydrogen to diffuse through the multilayers. Any inhomogeneous distribution of H in different Nb layers will, therefore, disappear in several minutes after charge at room temperature. The extra peak is thus believed to correspond to a second phase, instead of an inhomogeneous distribution in different Nb layers. From the phase diagram of the Nb-H system, the second phase at room temperature is expected to be ordered face-centered orthorhombic (fco) β hydride. Considering the decrease of the critical temperature for phase separation in thin films observed in Pd, the possibility may not be ruled out that the second phase here is α', a disordered condensed cubic hydride existing at higher temperature in bulk materials. Because of the small thickness of the layers and the fine grains in them, the diffraction peaks in the XRD spectra in reflectional as well as in tilting geometries are rather broad. This makes it impossible to distinguish between the α' phase and the β phase, the latter having splitted peaks around the former.[33]

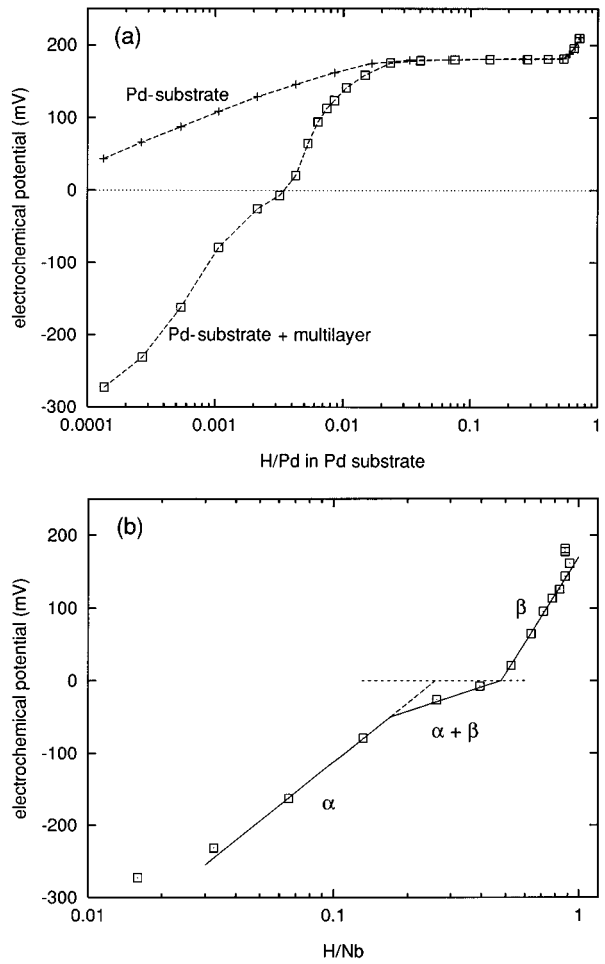

FIG. 8. Electrochemical potential vs H concentration at room temperature. (a) For a pure Pd substrate and for multilayers of $\Lambda=21$ nm on the same substrate vs total H concentration. (b) For the multilayers after substracting the H content within the Pd substrate in order to get the H concentration in the Nb layers of the multilayer. The three straight-line segments belong to the α and β single-phase regions and the two-phase region in between (reference: saturated calomel electrode).

The H content in Nb at which the phase separation occurs is always larger than in bulk Nb but has no obvious relation with Λ and cycle numbers.

From Fig. 7, it can be seen that the lattice parameters of both first and second phases are changing with the global hydrogen concentration. This is different from the case of bulk Nb where the concentration of coexisting phases and therefore their lattice parameters remain constant. Only the relative amount of each phase changes with global composition. A ''plateau'' with a remaining slope in the chemical potential-concentration relation results due to the change of compositions, as shown in Fig. 8(b). The sample used to get the results in Fig. 8 has a double-layer thickness of $\Lambda=21$ nm and a Nb layer thickness of 10.7 nm, similar to the corresponding values 28.3 nm and 13.6 nm for the multilayer in Fig. 7. A qualitative comparison of the results obtained by lattice parameter measurements in Fig. 7 and those by EMF measurements should be possible. If the three solid lines in Fig. 8(b) are associated with the α phase, the two-phase region, and the β phase, a phase separation occurs at H/Nb $=0.16$ and a potential of -50 mV. This terminal solubility is in agreement with the XRD measurements (see Fig. 7) where at the third loading an additional peak was detected at the same composition. Taking the potential of the saturated calomel electrode at a H_2 pressure of 1 atm as reference [230 mV (Ref. 23)], the potential value of -50 mV corresponds to a free enthalpy of solution of about 27 kJ/mol H which is in agreement with the bulk Nb value calculated from the plateau pressure.[34] At the end of the two-phase region, the potential has increased up to 0 mV which corresponds to a change of 50 mV or about 5 kJ/mol H. If this change of free enthalpy ΔG is attributed to internal stresses, a value of 3 GPa is calculated for the hydrostatic stress σ from the relation $\Delta G=\sigma V_H$, where V_H is the partial molular volume of H in Nb. The potential of 0 mV corresponds to a concentration ratio of H/Nb$=0.26$ in the α phase according to the extrapolated line of the α phase in Fig. 8(b). Thus the H concentration in the α phase increases from 0.16 to 0.26 within the two-phase region, in agreement with the change of lattice spacings in Fig. 7(b) showing an additional increase for the α phase within the miscibility gap.

From the results of the last section, it is known that the expansion of Nb layers are constrained by the substrate and neighboring Pd layers. Now let us consider the effects of this constraint on the phase separation of Nb hydride. A constraint energy term, W_C is added here into the simplified expression of the chemical potential of H, which was used to account for the phase separation in metal-H systems first by Lacher[35] and later by many investigators:[36]

$$\mu=\mu^0+RT\ln\left(\frac{\theta}{1-\theta}\right)+W_I\theta+W_C\theta, \tag{13}$$

where μ is the chemical potential of H, μ_0 is its value at standard state, θ is the fraction of interstices occupied in the bcc structure of Nb($X_H=6\theta$), and $W_I\theta$ is a term accounting for the long range attractive H-H interaction. The reason for a linear dependence of constraint energy on H concentration θ and the quantitative estimation of W_C are explained as follows.

As we did in the previous section, suppose first that the layer is expanded isotropically and freely upon absorption of H, with a relation described by Eq. (1) for Nb. Then a biaxial compressive stress is imposed elastically onto the film in its lateral directions to compensate exactly the expansion strain $\epsilon=\epsilon_{xx}=\epsilon_{yy}=K\theta$ due to H incorporation, where K is a constant being $K=0.058\times 6=0.348$ for Nb. Insert this strained layer into the multilayers and attach the package onto the substrate, an in-plane strain with $\epsilon=\epsilon_{xx}=\epsilon_{yy}=-0.348\theta$ and corresponding biaxial stress σ_{xx} and σ_{yy} are developed in the film. Using the isotropic approximation again, the stresses can be simply expressed by

$$\sigma=\sigma_{xx}=\sigma_{yy}=M\epsilon, \tag{14}$$

where

$$M=\frac{E}{1-\nu} \tag{15}$$

is the biaxial elastic modulus. The work required to put one mole H into a host with this stress field may be expressed by[23]

$$W=\tfrac{2}{3}M\epsilon V_H=\tfrac{2}{3}MK\theta V_H=W_C\theta, \tag{16}$$

where V_H is the partial molar volume of H in the host. W in Eq. (16) is the term we added for lateral constraint in Eq. (13). W_C is a constant which can be computed by Eq. (16).

Now that we have got the chemical potential of H, the critical temperature T_C, spinodal boundary θ_S, and phase boundary X_B could be calculated. With the same procedure used by Flanagan and Oates,[37] the first two parameters are obtained from Eq. (13) as follows:

$$T_c=-\frac{W_I+W_C}{4R}, \tag{17}$$

$$\theta_s=\frac{1}{2}\pm\frac{1}{2}\sqrt{1+\frac{4RT}{W_I+W_C}}. \tag{18}$$

As mentioned earlier, the H-H interaction is attractive in long range, thus W_I is negative. On the other hand, due to repulsive interaction of H with the compressive stress field, W_C is positive. Consequently T_C is decreased and the spinodal miscibility gap is narrowed, according to Eqs. (17) and (18). Now let us estimate the effect of the constraint on the critical phase separation temperature, T_C, in our case. From the experimental value of $T_C=444$ K for α-α' phase separation without constraint in bulk Nb,[38] $W_I=-15$ kJ/mol is obtained from Eq. (17) with $W_C=0$. From Eq. (16) and using the elastic constants of Nb,[26] W_C is estimated to be 65 kJ/mol. Thus we found a large negative critical temperature, indicating no phase separation could be reached if the film is really constrained completely in its lateral directions. Although it is a very crude estimation of T_C by Eq. (13), the above conclusion may be qualitatively valid considering the huge difference of W_I and W_C.

The above prediction contradicts obviously with the experimental observation that phase separation takes place in Nb layers of multilayers with the exception of one sample with a Nb layer thickness of 6.2 nm. However, if the stress imposed by the constraint of the substrate is relaxed by some mechanism like dislocation generation and glidding, the condition for the prediction will be lost. This may be quite realistic if the possible defects formed during the sample preparation process and the extra strain due to H incorporation are considered. The latter imposed a stress of the order of GPa. If the phase separation is initiated by the first elastic instability of the layers, the propagation of the second phase boundary could introduce even larger local stress and provide defect sources which catalyze further plastic flow. This may explain the above-observed contradiction. If the phase separation is initiated by plastic instability of the layers, its start will be controlled by a kinetic process like dislocation generation and movement. This depends strongly on local stresses and types of produced defects, instead of global thermodynamic factors, and makes the critical concentration for phase separation change irregularly. Another point is that the irreversible plastic flow can accommodate the strain of growth of a second phase and the layers in lateral directions can be strained again when H is removed quickly at higher temperature, as discussed previously. Also, when plastic flow occurs accompanying the phase separation, the local strain and stress is inhomogeneous and/or the stress may depend on the fraction of transformed Nb, which both could introduce compositional changes on a microscale level and thus, a slope of the chemical potential-H concentration plateau is expected, as seen in Fig. 8.

IV. SUMMARY

The behavior of H loading and unloading in Pd/Nb multilayers has been investigated. The elastic response of the Nb layers upon H absorption can be well described by a model assuming expansion in one dimension, based on bulk elasticity of Nb and the behavior of the bulk Nb-H system. The smaller expansion of the Nb layer in as-prepared samples is found to result from the relaxation of the strain developed during the preparation process of the sample by laser deposition. This relaxation is discussed based on the special defects formed in laser deposited films and their properties in a bcc structure. Phase separation is observed in the Nb and Pd layers probably initiated by plastic instability of the layers and introducing irreversible strain into the film. The latter remains in the film after H is released at higher temperature. A simple model is suggested to account for the effects of substrate constraints on phase separation of hydride in thin films or layered structures.

ACKNOWLEDGMENTS

The authors are grateful to Dr. D. Hesse and Dr. S. Senz at the Max-Planck-Institut für Mikrostrukturphysik in Halle for their help in XRD with Philips's X'pert. One of us, QMY, thanks the Alexander von Humboldt Foundation for financial support and Professor Dr. F. Sommer at the Max-Planck-Institut of Metals in Stuttgart, for the kind encouragement during QMY's stay in Stuttgart. Financial support by the Deutsche Forschungsgemeinschaft is gratefully acknowledged.

[1] P.F. Miceli, H. Zabel, and J.E. Cunningham, Phys. Rev. Lett. **54**, 917 (1985).
[2] P.F. Miceli and H. Zabel, Z. Phys. B **74**, 457 (1989).
[3] P.F. Miceli and H. Zabel, Phys. Rev. Lett. **59**, 1224 (1987).
[4] C. Uher, J. L. Cohn, P.F. Miceli, and H. Zabel, Phys. Rev. B **36**, 815 (1987).
[5] Y.Q. Sheng, P. Ziegler, E. Recknagel, O. Boebel, J. Steiger, and A. Weidinger, Phys. Rev. B **41**, 9794 (1990).
[6] B. Hjörvarsson, J. Rydén, E. Karlsson, J. Birch, and J.-E. Sundgren, Phys. Rev. B **43**, 6440 (1991).
[7] B. Hjörvarsson, M. Vergnat, J. Birch, J.-E. Sundgren, and B. Rodmacq, Phys. Rev. B **50**, 11 223 (1994).
[8] F. Stillesjö, B. Hjörvarsson, and B. Rodmacq, J. Magn. Magn. Mater. **126**, 102 (1993).

[9] P.M. Reimer, H. Zabel, C.P. Flynn, and J.A. Dura, Phys. Rev. B **45**, 11 426 (1992).
[10] F. Klose, J. Thiele, A. Schurian, O. Schulte, M. Steins, O. Bremert, and W. Felsch, Z. Phys. B **90**, 82 (1993).
[11] D. Nagengast, J. Erxmeyer, and A. Weidinger, J. Alloys. Comp. **231**, 307 (1995).
[12] A. Weidinger and H. Glückler, Philos. Trans. R. Soc. London Ser. A **350**, 277 (1995).
[13] M-W. Lee and R. Grosser, J. Appl. Phys. **57**, 5236 (1985).
[14] G.A. Frazier and R. Glosser, J. Phys. D **12**, L113 (1979).
[15] M. Nicolas, L. Dumoulin, and J.P. Burger, J. Less-Common Met. **130**, 61 (1987).
[16] E.M. Salomons, R. Feenstra, D.G. De Groot, J.H. Rector, and R. Griessen, J. Less-Common Met. **130**, 415 (1987).
[17] S. Moehlecke, C.F. Majkrzak, and M. Strongin, Phys. Rev. B **31**, 6804 (1985).
[18] J. Steiger, S. Blässer, O. Boebel, J. Erxmeyer, B. Mertesacker, and A. Weidinger, Z. Phys. Chem. (München) **181**, 942 (1993).
[19] P.M. Reimer, H. Zabel, C.P. Flynn, A. Matheny, K. Ritley, J. Steiger, S. Blässer, and A. Weidinger, Z. Phys. Chem. (München) **181**, 367 (1993).
[20] P.F. Miceli, H. Zabel, J.A. Dura, and C.P. Flynn, J. Mater. Res. **6**, 964 (1991).
[21] H.U. Krebs and O. Bremert, Appl. Phys. Lett. **62**, 234 (1993).
[22] M. Störmer and H.U. Krebs, J. Appl. Phys. **76**, 7080 (1995).
[23] R. Kirchheim, Prog. Mater. Sci. **32**, 261 (1988); R. Kirchheim, F. Sommer, and G. Schluckebier, Acta Metall. **30**, 1059 (1982).
[24] H. Wenzl, Int. Metall. Rev. **27**, 140 (1982).
[25] H. Peisl, in *Hydrogen in Metals I*, edited by G. Alefeld and J. Völkl, Topics in Applied Physics Vol. 28 (Springer-Verlag, Berlin, 1978), p. 53.
[26] D.I. Bolef, J. Appl. Phys. **32**, 100 (1961).
[27] S. Fähler and H.U. Krebs, Appl. Surf. Sci. (to be published).
[28] B.L. Eyre, M.H. Loretto, and R.E. Smallman, in *Vacancies '76*, edited by R.E. Smallman and J.E. Harris (The Metals Society, London, 1977), p. 63.
[29] W.D. Nix, Metall. Trans. A **20**, 2217 (1989).
[30] A.G. Evans and J.W. Hutchinson, Acta Metall. Mater. **43**, 2507 (1995).
[31] S. Amelinckx, in *Dislocations in Solids*, edited by F.R.N. Nabarro (North-Holland, Amsterdam, 1979), Vol. 2, p. 67.
[32] G. Schmitz, Q. M. Yang, Ph. Kesten, U. Geyer, U. V. Hirlsen, K. Reimann, and R. Kirchheim (unpublished).
[33] M.S. Rashid and T.E. Scott, J. Less-Common Met. **30**, 399 (1973).
[34] E. Fromm and E. Gebhardt, *Gase und Kohlenstoff in Metallen* (Springer-Verlag, Berlin, 1976), p. 461.
[35] J.R. Lacher, Proc. R. Soc. London Ser. A **161**, 525 (1937).
[36] T.B. Flanagan and W.A. Oates, in *Hydrogen in Intermallic Compounds I*, edited by L. Schlapbach, Topics in Applied Physics Vol. 63 (Springer-Verlag, Berlin, 1988), p. 49.
[37] W.A. Oates and T.B. Flanagan, J. Mater. Sci. **16**, 3235 (1981).
[38] H. Wagner, in *Hydrogen in Metals I* (Ref. 25), p. 5.